Research Square

Preprints are preliminary reports that have not undergone peer review.
They should not be considered conclusive, used to inform clinical practice,
or referenced by the media as validated information.

REAP1/AtSWAP70 Integrates RAB5 and ROP Signaling During Sexual Reproduction

Takashi Ueda

tueda@nibb.ac.jp

National Institute for Basic Biology https://orcid.org/0000-0002-5190-892X

Emi Ito

Ochanomizu University

Tomoko Hirano

Kyoto Prefectural University

Masa Sato

Kyoto Prefectural University https://orcid.org/0000-0001-5794-4545

Kazuo Ebine

National Institute for Basic Biology https://orcid.org/0000-0003-3020-7208

Akihiko Nakano

Live Cell Super-Resolution Imaging Research Team, RIKEN Center for Advanced Photonics
https://orcid.org/0000-0003-3635-548X

Tomohiro Uemura

Ochanomizu University https://orcid.org/0000-0001-7270-7986

Article

Keywords:

Posted Date: January 30th, 2025

DOI: https://doi.org/10.21203/rs.3.rs-5830709/v1

License: This work is licensed under a Creative Commons Attribution 4.0 International License.
Read Full License

Additional Declarations: There is **NO** Competing Interest.

Abstract

Small GTPases of the Ras superfamily are critical regulators of diverse cellular processes. While cross-talk between their signaling pathways has been documented in animals, similar mechanisms remain unexplored in plants, where small GTPases have undergone unique evolutionary diversification. Here, we identify REAP1/AtSWAP70 as a novel effector in *Arabidopsis thaliana* that interacts with the active forms of both canonical RAB5 and the plant-specific RAB5, ARA6. Remarkably, REAP1 also binds to active ROP7, a plant-unique Rac-type GTPase, via its DH domain. REAP1 localizes to endosomes and facilitates ROP7 recruitment from the plasma membrane, a process dependent on RAB5 activity. Genetic analyses reveal that the RAB5-REAP1-ROP7 signaling cascade is essential for gametogenesis, impacting pollen viability and development. This study provides the evidence of functional cross-talk between RAB and ROP signaling in plants, unveiling a novel layer of regulatory complexity in plant GTPase signaling during plant reproduction.

Introduction

Small GTPases of the Ras superfamily are critical regulators of diverse cellular processes, acting as molecular switches that alternate between active, GTP-bound states and inactive, GDP-bound states. This cycling is regulated by guanine nucleotide exchange factors (GEFs), which promote GDP-GTP exchange, and GTPase-activating proteins (GAPs), which stimulate GTP hydrolysis. Upon activation, conformational changes in the switch I and II regions enable small GTPases to interact with effector proteins, initiating specific downstream signaling pathways [1].

The Ras superfamily comprises five major subfamilies: Ras, Rho/Rac/Cdc42, Rab, Sar/Arf, and Ran [2]. Each subfamily specializes in distinct cellular functions: Ras regulates cell proliferation and differentiation, Rho controls cytoskeletal organization and polarity, Rab and Sar/Arf mediate membrane trafficking, and Ran facilitates nuclear transport. Crosstalk between these subfamilies often supports complex cellular functions, as observed in animal systems. For instance, Ras and Rho pathways interact to remodel the actin cytoskeleton and enhance cell motility in oncogenic RAS-transformed fibroblasts [3]. Coordination between Rab and Rho pathways has been implicated in neurodegenerative diseases, where disrupted cytoskeletal dynamics and membrane trafficking contribute to pathogenesis [4]. However, the integration of small GTPase pathways in plants remains largely unexplored, mainly due to unique features of plant small GTPases.

Although small GTPase families are broadly conserved across eukaryotes, plants exhibit unique adaptations. The Ras subfamily, critical for cell proliferation in animals, was lost in plants during evolution, while the Rab and Rho families underwent significant diversification. In *Arabidopsis thaliana*, the Rab family includes 57 members, comparable to the 60 in humans. However, plant Rabs are classified into only eight subgroups, differing from the 39 in humans [5]. Plants lack certain Rab subgroups found in animals, such as Rab4, which mediates endosome-to-plasma membrane (PM) recycling, and Rab9, which regulates endosome-to-TGN transport [6,7]. Instead, plants have uniquely

expanded Rab subgroups, such as RAB11, which includes 26 members in Arabidopsis compared to two in humans [8]. The plant-specific ARA6 subgroup of RAB5, coexisting with canonical RAB5, exemplifies further unique diversification of the Rab group [9,10]. ARA6 has distinct structural features and regulates different endosomal trafficking pathways from canonical RAB5, partially counteracting canonical RAB5 [11–14].

The Rho family exhibits similar plant-specific adaptations. While animals and yeast possess three subfamilies (Rac, CDC42, and Rho), plants lack Rho and CDC42 homologs, instead harboring a unique ROP (Rho of Plants) family, most similar to Rac [15]. Plant ROPs regulate diverse processes, including tip growth of pollen tubes and root hairs, immune responses, leaf pavement cell morphogenesis, auxin-dependent polar growth, xylem pit formation, cell division through cytoskeletal reorganization and plant-microbe interactions [16–18]. ROPs are activated by multiple GEF types, including PRONE domain-containing ROP GEFs unique to plants, and a small number of DBL-type Rho GEFs, which include homologs of SWAP70 [15,16,18].

DBL-type Rho GEFs are defined by their Dbl homology (DH) domain, which confers GEF activity, and a pleckstrin homology (PH) domain, required for phosphoinositide binding [19]. In *Oryza sativa*, SWAP70 has been shown to activate OsRac1, contributing to immune responses against chitin elicitors [20]. In Arabidopsis, the homolog AtSWAP70 also contains a DH domain, but its specific role in ROP activation remains unclear.

Despite the biological importance of Rab and ROP GTPases, whether their functions are integrated in plants has remained unknown. In this study, we identified RAB5 EFFECTOR OF ARABIDOPSIS WITH PH DOMAIN 1 (REAP1)/*Arabidopsis thaliana* SWITCHING B-CELL COMPLEX ASSOCIATED (AtSWAP70) as a novel effector that interacts with active canonical RAB5 and ARA6. We also discovered that REAP1 binds to the active form of ROP7, but not to the inactive form, and facilitates its recruitment to endosomes under the regulation of RAB5. Further investigation revealed that this RAB5-REAP1-ROP7 cascade is involved in pollen development and gametophyte function. Our findings uncover a previously unrecognized mechanism integrating Rab and ROP signaling in plants, with potential implications for understanding plant-specific adaptations of small GTPase-mediated signaling.

Results

REAP1 interacts with both plant-specific and canonical RAB5s

To better understand the molecular functions of plant RAB5, we focused on PH domain-containing proteins, as these proteins are often involved in membrane trafficking [21–23]. The Arabidopsis genome encodes 53 PH domain-containing proteins [21]. To investigate whether any of these proteins interact with ARA6, we performed a yeast two-hybrid screen using the constitutively active form of ARA6 ($ARA6^{Q93L}$)

as bait. This screening identified AT2G30880 as a novel effector candidate for ARA6, which we named REAP1 (Fig. 1a).

To determine whether REAP1 interacts with ARA6 in a nucleotide-state-dependent manner, the interactions of REAP1 with the wild-type, constitutively active ($ARA6^{Q93L}$), and dominant-negative ($ARA6^{S47N}$) forms of ARA6 were tested. REAP1 interacted with the wild-type and constitutively active forms but not with $ARA6^{S47N}$ (Fig. 1a). Next, we tested whether REAP1 also interacts with ARA7, a canonical RAB5 in Arabidopsis. Similar to its interaction with ARA6, REAP1 interacted with the wild-type and constitutively active forms of ARA7 ($ARA7^{Q69L}$) but not with the dominant-negative form ($ARA7^{S24N}$) (Fig. 1a).

To confirm these interactions, we conducted pull-down assays. HA-tagged REAP1 expressed in yeast was pulled down by bacterially expressed and purified GST-tagged $ARA6^{Q93L}$ and $ARA7^{Q69L}$, but not by GST-tagged $ARA6^{S47N}$ or GST-$ARA7^{S24N}$ (Fig. 1b). These findings indicate that REAP1 interacts with these both ARA6 and canonical RAB5 in their GTP-bound states and functions as an effector for these RAB5 proteins.

REAP1 Binds to PI3P and PI3,5P2

Given the known role of the PH domain in phosphoinositide interactions, we investigated whether REAP1 binds to specific phosphoinositides. An overlay assay using bacterially expressed and purified GST-REAP1 revealed that REAP1 specifically binds to phosphatidylinositol 3-phosphate (PI3P) and phosphatidylinositol 3,5-bisphosphate (PI3,5P2) (Fig. 1c).

To assess the functional relevance of these interactions, we examined the effects of wortmannin (Wm), a phosphatidylinositol-3 and − 4 kinase inhibitor [24–28], and YM201636, an inhibitor of PI3P-5-kinase a FYVE-type zinc finger containing (PIKfyve) also known as Formation of aploid and binucleate cells 1 (FAB1) [29,30], on the subcellular localization of REAP1. Transgenic plants expressing mGFP-tagged REAP1 under the control of its native regulatory elements (promoter, introns, and terminator) in a *reap1* mutant background were treated with these inhibitors. In mock-treated cells, mGFP-REAP1 localized to punctate organelles (Fig. 1d). Upon Wm treatment, mGFP-REAP1 was dispersed into the cytosol. In contrast, YM201636 treatment did not completely alter the subcellular distribution of GFP-REAP1 in root epidermal cells, although the number of puncta labeled by GFP-REAP1 was significantly reduced in cortex cells (Fig. 1e). These findings suggest that PI3P and PI3,5P2 are important for regulating the subcellular localization of REAP1.

REAP1 Colocalizes with Canonical RAB5 and ARA6 on Endosomes

To determine the organelle where REAP1 localizes, we compared its subcellular distribution with several organelle markers. REAP1 exhibited strong colocalization with both RAB5 members and VPS9A, the

common activator of plant-specific and canonical RAB5s (Fig. 2a) [31]. However, REAP1 did not colocalize with markers for the *trans*-Golgi network (VHAa1-mRFP) [32] or *trans*-Golgi cisternae (ST-mRFP) [33] (Extended Data Fig. 1). These results suggest that REAP1 localizes to multivesicular endosomes (MVEs) together with RAB5s and their activator VPS9A.

To investigate whether REAP1-labeled MVEs are sensitive to brefeldin A (BFA), an ARF GEF inhibitor [34,35], we treated plants co-expressing GFP-REAP1 and mRFP-tagged RAB5s with BFA. MVEs are known to form aggregates called BFA bodies upon BFA treatment [36]. Given that REAP1 localizes to MVEs, we sought to determine whether REAP1-bearing MVEs also exhibit sensitivity to BFA. While ARA6- and ARA7-bearing MVEs aggregated into BFA bodies in response to treatment, REAP1-labeled compartments were not incorporated into these BFA bodies (Fig. 2b). This finding suggests that REAP1 localizes to a subset of MVEs that are less sensitive to BFA.

Endosomal localization of REAP1 requires RAB5 activity

To determine whether the endosomal localization of REAP1 depends on RAB5 activity, we examined the subcellular localization of GFP-REAP1 in the *ara6-1* [14] and *vps9a-2* [31] mutants. In the *ara6-1*mutant, GFP-REAP1 localized to punctate organelles similar to the pattern observed in the wild type (Fig. 2c). In contrast, in the *vps9a-2* mutant, GFP-REAP1 was dispersed in the cytosol and partially mislocalized to the vacuolar membrane (Fig. 2c, arrowheads).

VPS9A is a common activator of ARA6 and canonical RAB5, promoting their recruitment to MVEs [31]. The altered localization of REAP1 in the *vps9a-2* mutant led us to hypothesize that canonical RAB5, but not ARA6, determines the subcellular localization of REAP1. To test this hypothesis, we performed a transient expression experiment using Arabidopsis root cultured cells [11]. GFP-REAP1 localized to punctate organelles overlapping with MVE markers, tagRFP-ARA7 and ARA6-tagRFP. A similar localization pattern was observed in cells expressing constitutively active forms of canonical RAB5 ($ARA7^{Q69L}$) and ARA6 ($ARA6^{Q93L}$). In contrast, when dominant-negative ARA7 ($ARA7^{S24N}$) was overexpressed, GFP-REAP1 was not detected on punctate compartments and instead appeared dispersed in the cytosol. However, the expression of dominant-negative ARA6 ($ARA6^{S47N}$) did not affect the subcellular localization of GFP-REAP1 (Fig. 2d). These findings support the hypothesis that the MVE localization of REAP1 is specifically regulated by canonical RAB5.

REAP1 interacts with active ROP7

Previous studies reported that rice OsSWAP70, orthologous to REAP1, activates OsRac1 and that OsSWAP70 and OsRac1 function cooperatively during pathogen responses [20]. To investigate whether REAP1 interacts with ROP members in Arabidopsis, we performed yeast two-hybrid assays to test

interactions between REAP1 and the 11 Arabidopsis ROP members (Extended Data Fig. 2). The results showed that REAP1 interacts with both the wild-type and constitutively active forms of ROP7.

It has also been reported that a DH domain-like sequence is present in the amino acid region 203–401 of REAP1 (Fig. 3a) [37]. To determine whether this DH domain-like sequence is required for the interaction between REAP1 and ROP7, we conducted a domain dissection analysis (Fig. 3b). Yeast two-hybrid analysis revealed that the DH domain-like region of REAP1 is necessary and sufficient for its interaction with the constitutively active form of ROP7.

Similarly, to identify the regions of REAP1 required for its interaction with RAB5, we performed a domain dissection analysis. The results showed that the active form of ARA6 interacts with the sequence containing the DH domain along with its flanking regions, whereas the active form of ARA7 was able to interact with the DH domain alone (Fig. 3c). These results suggest that the DH domain of REAP1serves as a critical interface for both RAB5 and ROP7.

Next, we examined the interaction between REAP1 and ROP7 in vivo by a bimolecular fluorescence complementation (BiFC) assay. Full-length REAP1 was fused to the N-terminal portion of VENUS (nVENUS), and wild-type ROP7 was fused to the C-terminal portion of VENUS (cVENUS). When these constructs were transiently expressed in tobacco leaf epidermal cells, reconstituted VENUS fluorescence was observed, indicating an interaction between REAP1 and wild-type ROP7 (Fig. 3d). Fluorescence was also detected with the combination of REAP1 and the constitutively active form of ROP7. In contrast, no fluorescence was observed for combinations of REAP1 and the dominant-negative form of ROP7, REAP1 and wild-type ROP1, or REAP1 and wild-type ROP2 (Fig. 3d).

We then examined the intracellular distribution of the reconstituted VENUS fluorescence resulting from the interaction between nVENUS-REAP1 and cVENUS-ROP7. The fluorescence was observed to localize to both the PM of epidermal cells and punctate structures within the cytoplasm (Fig. 3e). These punctate structures were highly mobile along the cytoplasmic streaming (Fig. 3f, Extended Data Movie 1, Extended Data Movie 2, and Extended Data Movie 3).

Overexpression of REAP1 and RAB5s recruit ROP7 to endosomes

Many Arabidopsis ROP members have been reported to localize predominantly to the PM [38,39]. Since REAP1 localizes to MVEs and interacts with ROP7 at punctate structures, we hypothesized that REAP1 might recruit ROP7 to MVEs. To test this, we examined the effect of REAP1 overexpression on the subcellular localization of ROP7. When wild-type ROP7 was transiently expressed in tobacco epidermal cells, it localized predominantly to the PM. In some cells, ROP7 was also concentrated in the nucleus and nucleolus. Upon co-expression with REAP1, a subpopulation of ROP7 remained at the PM, while co-localization of REAP1 and ROP7 was observed in punctate structures where REAP1 localized (Fig. 4a).

Interestingly, the constitutively active form of ROP7 localized to both the PM and punctate structures even without co-expression of REAP1. These cytosolic punctate structures were also labeled by REAP1. In contrast, the dominant-negative form of ROP7 localized only to the PM, with no recruitment to punctate structures observed upon co-expression with REAP1. Similarly, wild-type ROP1 and wild-type ROP2 also localized to the PM in the absence of REAP1 co-expression, and no recruitment to punctate structures was observed with REAP1 co-expression. Furthermore, REAP1 overexpression did not affect the localization of the PM marker SYP132 (Extended Data Fig. 3a).

Given that REAP1 is an effector downstream of RAB5, we predicted that RAB5 overexpression would affect the subcellular localization of ROP7 similarly to REAP1 overexpression. To test this, we performed experiments analogous to those conducted for REAP1 overexpression (Fig. 4b). The results showed that overexpression of wild-type ARA7 or wild-type ARA6 resulted in the recruitment of wild-type ROP7 to MVEs where RAB5 is localized. This effect was not observed with overexpression of RAB11s (RABA1b or RABA6a), nor with overexpression of another MVE marker, VAMP727 (Extended Data Fig. 3b). These findings suggest that both RAB5 and REAP1 play a role in the recruitment of ROP7 to endosomes.

RAB5, REAP1 and ROP7 act in a cascade to recruit ROP7 to endosomes

To determine whether REAP1 is involved in RAB5-mediated recruitment of ROP7 to endosomes, we examined the subcellular localization of ROP7 in *reap1* mutant root protoplasts. We successfully detected GFP signals in protoplasts prepared from transgenic plants expressing GFP-REAP1 under the control of its native promoter in the *reap1* mutant background, confirming REAP1 expression in root protoplast cells (Extended Data Fig. 4a). The punctate localization of GFP-REAP1also confirms that the protoplast preparation process has negligible effects on its subcellular localization. When tagRFP-tagged ARA7 was expressed under the control of the 35S promoter, ARA7 localized to enlarged ring-shaped endosomes in this system (Extended Data Fig. 4b).

Next, we compared the subcellular localization of ROP7 in wild-type and *reap1* mutant protoplasts. In both genotypes, ROP7 predominantly localized to the PM under basal conditions (Extended Data Fig. 4c). However, upon overexpression of ARA7 in wild-type protoplasts, ROP7 exhibited a punctate localization pattern, with GFP-ROP7 signals within ring-like endosomes formed by ARA7 overexpression (Fig. 5). In contrast, in *reap1* mutant protoplasts, ARA7 overexpression resulted in the formation of enlarged ring-like endosomes, but ROP7 failed to associate with these structures (Fig. 5).

These results suggest that REAP1 mediates the action of ARA7 in the recruitment of ROP7 to MVEs, forming a RAB5-REAP1-ROP7 signaling cascade.

RAB5-REAP1-ROP7 cascade is required for gamete development

To investigate the role of the RAB5-REAP1-ROP7 cascade in plant growth and development, we analyzed the phenotype of the *reap1* mutant (Fig. 5a, Extended Data Fig. 5a). Under standard laboratory conditions, no macroscopic differences were observed between *reap1* and wild-type plants. We then obtained the *rop7* mutant and generated the *reap1 rop7*double mutant through crossing. The *rop7* mutant harbors a T-DNA insertion in the sixth intron (Extended Data Fig. 6a), and RT-PCR and real-time PCR analyses confirmed that *ROP7* expression was reduced to approximately one-tenth of the wild-type level (Extended Data Fig. 6b), indicating that it is a knockdown mutant. Phenotypic observations revealed no significant differences between the *rop7* or *reap1* single mutants and the wild type. Similarly, the *reap1 rop7* double mutant exhibited no obvious macroscopic abnormalities under normal growth conditions (Fig. 6a).

We next examined the genetic interaction between *REAP1* and *RAB5*. The *vps9a-2* mutant, a weak allele mutant of *VPS9A* encoding the major activator for all three RAB5 members in *Arabidopsis*, exhibits multiple phenotypic defects, including impaired primary root elongation [31]. Previous studies have shown opposing effects of mutations in canonical (*ARA7* and *RHA1*) and plant-specific RAB5 (*ARA6*) on the *vps9a-2* phenotype; the abnormalities of *vps9a-2* are exacerbated by *ara7*, but suppressed by the *ara6* mutation [14]. The hemizygous mutation in *PUF2* for a regulator of RAB5-mediated endosomal transport also exaggerates the *vps9a-2* mutation [13]. Based on these findings, we investigated how the *reap1* mutation affects the *vps9a-2* phenotype. Interestingly, the *reap1* mutation partially suppressed the *vps9a-2* phenotype (Fig. 6b). This suppression was completely abolished when a genomic fragment of *REAP1* or GFP-tagged *REAP1* was introduced into the *reap1 vps9a-2* double mutant (Extended Data Fig. 5b,c), confirming that the suppression was due to the *reap1* mutation.

We then analyzed the genetic interaction between *ROP7* and *VPS9A*. Notably, we were unable to recover the *rop7 vps9a-2*double mutant. Although *ROP7* and *VPS9A* are located on different chromosomes, self-pollination of *rop7*$^{+/-}$ *vps9a-2*$^{+/-}$ heterozygous plants failed to produce *rop7*$^{-/-}$ *vps9a-2*$^{+/-}$ or *rop7*$^{+/-}$ *vps9a-2*$^{-/-}$ progeny (Extended Data Table 1, Table 2). To investigate this further, we constructed a DNA fragment to express mGFP-tagged *ROP7* under the control of its native promoter (Extended Data Fig. 6c) and introduced it into *rop7*$^{+/-}$ *vps9a-2*$^{+/-}$. In the T2 generation, we successfully obtained transformants expressing mGFP-ROP7 in the *rop7-/- vps9a-2+/-* background (Extended Data Fig. 6d,e). These results suggest that the combination of *rop7* and *vps9a-2* mutations impairs gametophyte function.

To test this hypothesis, we performed cross-pollination experiments (Extended Data Table 3). When *rop7*$^{+/-}$ *vps9a-2*$^{+/-}$ plants were crossed with wild-type plants, the *rop7 vps9a-2* mutant combination was not transmitted to the next generation, regardless of whether the mutant plant was used as the female or male parent. This observation suggests that *ROP7* and *VPS9A* function cooperatively in both male and female gametophyte development. To investigate this further, we focused on pollen development and generated the *qrt1-4 rop7*$^{+/-}$ *vps9a-2*$^{+/-}$ mutant for detailed analysis (Fig. 6c). The *qrt1-4* mutant (control), as well as the *qrt1-4 rop7* and *qrt1-4 vps9a-2* mutants, formed normal pollen tetrads whose viability was confirmed by Alexander staining [40]. In contrast, pollen from *qrt1-4 rop7*$^{+/-}$ *vps9a-2*$^{+/-}$ plants exhibited

notable abnormalities. Approximately half of the tetrads (51.3%) were similar to the control. Among the others, the majority of tetrads showed a 1:1 ratio of normal to aborted pollen grains (43.0%), while a small population contained three (3.2%) or four (2.5%) aborted pollen grains per tetrad (Fig. 5c). This result indicates that ROP7 and normal RAB5 activation are essential for gametophyte development after meiosis, and the *rop7 vps9a-2* mutation may affect the development of microspores with a wild-type genotype within the tetrad.

Although the *reap1 rop7* and *reap1 vps9a-2* double mutants were successfully obtained, significantly higher proportions of aborted pollen grains (0.79% for *reap1 rop7* and 1.78% for *reap1 vps9a-2, P* < 0.01, Fisher's exact test) were observed in the pollen population from these mutants compared to the wild type (0.14%) (Extended Data Fig. 7). These findings suggest that REAP1 is required for the full functionality of ROP7 to cooperate with RAB5 during pollen development.

Discussion

Crosstalk between distinct small GTPase families in plant

Small GTPases are key regulators of various cellular processes, but how their functions are integrated during developmental processes in plants remains unexplored. In this study, we identified REAP1 as a novel effector for both the canonical RAB5 and ARA6 in Arabidopsis. We also found that REAP1 interacts with the constitutively active form of ROP7 and facilitates the recruitment of active ROP7 to endosomes. Similarly, RAB5 promotes ROP7 recruitment to endosomes, and this process depends on REAP1. These findings reveal the existence of a RAB5-REAP1-ROP7 signaling cascade in Arabidopsis, in which ROP7 functions on endosomes to regulate developmental processes, including pollen development (Fig. 5d). This study demonstrates the functional interplay between two distinct types of small GTPases, RAB and ROP, in plants. Crosstalk between different small GTPase subfamilies has been previously reported in animal systems [3,4]. However, the cascade we identified involves ARA6, a plant-specific RAB5 GTPase uniquely acquired during plant evolution, alongside ROPs, which are uniquely diversified in plants, and canonical RAB5. This suggests that this regulatory system was specifically adapted in plants. Our findings underscore the universal importance of integrative interactions among different types of small GTPases, while also highlighting the plant-specific adaptations of small GTPase cascades shaped during evolution.

REAP1 interacts with active ROP7

REAP1 was previously identified as AtSWAP70 [37], a protein whose rice homolog has been reported to function as a guanine nucleotide exchange factor (GEF) for OsRac1. This homolog plays a critical role in immune responses, including defense gene expression and reactive oxygen species (ROS) production in response to chitin elicitors [20]. Similar to its rice counterpart, AtSWAP70 contains the DH domain, known to activate Rho GTPases in animal systems, suggesting that AtSWAP70 might also possess ROP GEF activity. However, our findings indicate that AtSWAP70 interacts specifically with the GTP-bound form of

ROP7, and the DH domain alone is sufficient for this interaction (Fig. 3b). Given that GEFs typically interact with GTPases in their inactive GDP-bound state, our results suggest that the DH domain of AtSWAP70 may not function as a GEF, but may have evolved to serve as an interaction site with ROP proteins. This hypothesis warrants further experimental validation. Another intriguing question is whether REAP1 can simultaneously interact with both RAB5 and ROP7 or if their binding is competitive. Our data suggest that RAB5 binds to REAP1 at its DH domain, raising the possibility of distinct or overlapping interaction mechanisms.

It has been reported that ROP7 is activated by ROP GEF2 and ROP GEF4 to regulate stomatal behavior [41]. Additionally, ROP GEF8, which is activated by phosphatidic acid, also activates ROP7 [42]. Notably, ROP GEF8 interacts with both canonical RAB5 and ARA6, regardless of their nucleotide-binding states, and cooperatively regulates pollen tube germination with ROP1 (personal communication, Yan Zhang). This group also discovered that ARA6 and canonical RAB5 act synergistically during pollen germination, unlike their counteracting functions during vegetative development. These findings suggest that crosstalk between RAB5 and multiple ROP proteins forms an integral and specific mechanism underlying various reproductive processes. Exploring this mechanism further will be an exciting avenue for future research.

Physiological roles of plant RAB5-REAP1-ROP7 cascade

ROP7 has been reported to exhibit high expression during xylem differentiation, where it regulates the density of cell wall bands in protoxylem cells [15,43,44]. Additionally, ROP7 is expressed in guard cells, where it is activated by ROP GEF2 through interactions with PHYB, playing a downstream role in red light-induced stomatal opening [41]. In this study, we uncovered a novel role for ROP7 in the development of both male and female gametophytes.

Notably, the segregation ratios of offspring from *rop7*$^{+/-}$ *vps9a-2*$^{+/-}$ mutant plants did not statistically support any of the three hypotheses we tested: (1) a 15:1 segregation ratio in double mutants, (2) lethality in either male or female gametophytes, or (3) lethality in both male and female gametophytes (Extended Data Table 2). These findings suggest that the phenotypic abnormalities observed are not solely attributable to gametophyte lethality. When combined with the results of the pollen viability assay, our data indicate that the *rop7 vps9a-2* mutation results in complex phenotypic abnormalities, including effects on microspores within the same tetrad.

Regarding ROP7's role in female gametophyte formation, previous studies have reported its expression in synergid cells [45], implicating ROP7 in synergid cell functions. To further elucidate the physiological significance of the RAB5-REAP1-ROP7 cascade during gametogenesis, future studies should include detailed phenotypic analyses of *rop7*$^{+/-}$ *vps9a-2*$^{+/-}$ gametophytes and observations of ROP7, REAP1, and RAB5 dynamics throughout gametophyte development.

Implications of endosomal recruitment of ROP7

Although ROP7 has been reported to localize to the PM [46,47], its roles in endosomal functions have not been explored until now. In this study, we found that ROP7, but not ROP1 or ROP2, is recruited to endosomes via the expression of REAP1 or canonical RAB5. Since ROP7 interacts with REAP1 in its GTP-bound active state, it is possible that ROP7 initiates downstream signaling at endosomes, which may be critical for normal gametogenesis. However, the precise molecular mechanisms and biological significance of such endosomal signaling remain less understood in plants. Alternatively, endosomal recruitment of ROP7 could serve as a mechanism to downregulate its signaling activity. At the PM, ROP7 has been implicated in regulating the density of cell wall bands in protoxylem cells through interactions with ROP GAPs and ROP GEFs [44]. Thus, recruitment of active ROP7 to endosomes may attenuate its functional activity at the PM. It is also possible that recruitment of active ROP7 followed by ESCRT-mediated protein sorting at MVEs serves to degrade active ROP7. In our protoplast experiments, ROP7 was detected enclosed within the enlarged endosomes induced by ARA7 expression. Future research focusing on the downstream signals of the RAB5-REAP1-ROP7 cascade will be crucial to elucidate the biological significance of this novel intracellular signaling unit in plants.

Materials and Methods

Plasmid construction for yeast two-hybrid and BiFC experiments

For yeast two-hybrid experiments, the full-length complementary DNA (cDNA) sequence of *REAP1* was cloned into the pAD-GAL4-GWRFC vector provided by Dr. Demura (NAIST, Japan) using the Gateway cloning technique (ThermoFisher Scientific). The cDNA sequences encoding constitutively active (QL) and dominant negative (SN) forms of ARA6 and ARA7 were cloned into the *SalI* site of the pBD-GAL4-Cam vector (Agilent Technologies, Santa Clara, California, USA). Truncated REAP1 fragments were amplified using the primer sets listed in Extended Data Table 4 and subsequently cloned into pAD-GAL4-GWRFC using the gate way cloning technique. Arabidopsis *ROP* coding sequences were amplified from open flower or root cDNA libraries and cloned into pBD-GAL4-GWRFC, also provided by Dr. Demura, using the Gateway cloning technique. Constitutively active (GV) and dominant negative (TN) forms of *ROP*s [38,48] were generated by PCR-based site-directed mutagenesis using the primers listed in Extended Data Table 4.

For BiFC vector construction, cDNA sequences of REAP1, ROP7, ROP7^{G15V}, ROP7^{T20N}, ROP1, and ROP2 were first cloned into pENTR/D-TOPO using the Gateway TOPO reaction. The resulting constructs were digested with *EcoRV* and subsequently transferred into pDEST-VYCE(R)^{GW} and pDEST-VYNE(R)^{GW} vectors [49] using Gateway LR reactions.

Yeast two-hybrid interaction assay

Individual interaction assays were performed using GAL4 two-hybrid phagemid vector kits (Agilent Technologies) and strain AH109 (Takara Clontech, Kusatsu, Shiga, Japan). Colonies were grown in

selective medium lacking leucine and tryptophan (-LW), diluted to OD600 of 0.5 for testing interactions between REAP1 and RAB5s, or to OD600 of 1.8 for testing interactions between REAP1 and ROPs. Cultures were spotted onto plates lacking leucine, tryptophan, and histidine (-LWH).

Expression and purification of recombinant proteins

$ARA6^{Q93L}$, $ARA6^{S47N}$, $ARA7^{Q69L}$, $ARA7^{S24N}$, and REAP1 were expressed as glutathione S-transferase (GST)-fusion proteins using the pGEX6P-1 vector (GE Healthcare, Little Chalfont, Buckinghamshire, England). GST-RAB5 was expressed in *Escherichia coli* strain DH5α, and GST-REAP1 was expressed in Rosetta-gami™ 2 (DE3) (Merck, Darmstadt, Germany). The recombinant proteins were then purified according to the manufacturer's instructions.

In vitro pull-down assay

HA-tagged REAP1 was expressed in yeast strain YPH414 (MATa Δpep4:TRP1 *ura3 lys2 ade2 trp1 his3 leu2*) under the control of the GAL1 promoter. Yeast cells were collapsed by vertexing with glass beads in PSB supplemented with a protease inhibitor cocktail (cOmplete, EDTA-free, Merck). The collected cell lysate was mixed with 0.2 nmol GST or GST-tagged RAB5 proteins prebound to glutathione-Sepharose 4B resin. The mixture was incubated for 60 minutes at 4 ℃ in binding buffer [PBS buffer containing 0.05% Tween-20 and protease inhibitor cocktail (Merck)]. After incubation, the beads were washed three times with binding buffer, and the bound proteins were subjected to immunoblotting analysis.

Lipid-binding assay using PIP Strips

PIP strips (Echelon Biosciences Inc., Salt Lake City, Utah, USA) were blocked overnight at 4 ℃ in TBS buffer [25 mM Tris-HCl pH7.4, 137 mM NaCl, 2.68 mM KCl] containing 3% fatty acid-free BSA (Wako Fujifilm, Osaka Japan). After blocking, the strips were incubated with 10 nM GST or GST-REAP1 in TBS-T (TBS with 0.1% Tween-20) for 1 hour at room temperature with gentle agitation. After incubation, the strips were washed three times for 15 minutes each in TBS-T with gentle agitation. The strips were then incubated with anti-GST antibody (Santa Cruz Biotechnology, Santa Cruz, California, USA) diluted 1:1000 in TBS-T for 1 hour at room temperature with gentle agitation. After three washes with TBS-T, the strips were incubated with anti-rabbit HRP-conjugated secondary antibody diluted 1:10000 in TBS-T for 1 hour at room temperature. The strips were washed three more times and signals were detected using a chemiluminescent reagent (Immobilon ^{TM} Western Chemiluminescent HRP Substrate; Millipore, Burlington, Massachusetts, USA).

Generation of transgenic plants

Translational fusions between cDNAs for fluorescent proteins and Arabidopsis genes were generated using fluorescent tagging of full-length proteins. Briefly, the cDNA for monomeric GFP (mGFP) or mRFP were inserted in front of the start or stop codon of each gene with the following flanking sequences: 2055 kbp 5' and 996 kbp 3' for *REAP1*, and 1973 bp 5' and 1015 bp 3' for *ROP7*. The primer sequences used to amplify genomic REAP1 and genomic ROP7 sequences are listed in Extended Data Table 4. The

resulting DNA fragment was subcloned into the pGWB1 vector, kindly provided by Dr. Nakagawa (Shimane University, Japan). For the *reap1* complementation assay, a genomic fragment including *REAP1* and the same 5' and 3' flanking sequences was subcloned into pGWB1, and transformed into *reap1 vps9a-2* double mutant. For the *rop7* complementation assay, *pROP7*::mGFP-ROP7 sequence was similarly subcloned into pGWB1. The construct was first transformed into *rop7*$^{+/-}$ *vps9a-2*$^{+/-}$ double mutant, and the genotypes of the T2 lines were confirmed by PCR-based genotyping to validate complementation. Arabidopsis plants were transformed using the floral dip method with Agrobacterium tumefaciens strain GV3101:pMp90. Transgenic lines with a 1:3 segregation ratio for antibiotic resistance were selected, indicating a single-locus insertion of the transgene. These lines were used for subsequent experiments.

Plant materials and growth conditions

Arabidopsis thaliana Columbia-0 (Col-0) was used as the wild-type in all experiments. The T-DNA insertion line *reap1/atswap70* (GABI_096E03) was provided by Dr Yamaguchi and Dr Kawasaki (Kinki University, Japan)[37]. The *rop7* mutant (SALK_041927) was obtained from the Arabidopsis Biological Resource Center (ABRC) and backcrossed three times with wild type Col-0 before using for the experiments. Other mutant lines, *vps9a-2* (GABI_557C02) [31], *ara6-1* (SAIL_880-C07) [14], *puf2* (SAIL_24_C10) [13] and *qrt1-4* (SALK_024104) [50], and the transgenic lines expressing mRFP-ARA7 [51], ARA6-mRFP [14], VPS9A-GFP [31],VHAa1-mRFP [32] and ST-mRFP [33] have been described previously. Seeds were surface sterilized by exposure to 70% ethanol for 5 minutes with gentle agitation, followed by rinsing with 100% ethanol. Sterilized seed were plated on half-strength Murashige & Skoog (MS) medium including vitamins (Duchefa Biochemie, Haarlem, Netherlands), 1% sucrose, 0.5% MES-KOH (pH 5.8), and 0.5% (w/v) gellan gum (Wako Fujifilm) for observation by confocal laser scanning microscopy, or 1% (w/v) gellan gum for experiments examining overall macroscopic phenotypes and primary root elongation. Plates were incubated at 4°C for 2 days for stratification and then transferred to a growth chamber maintained at 22°C under long-day condition (16-hour light/8-hour dark). After 14 days, seedlings were transferred to soil and grown at 22°C under the same long-day conditions.

Microscopy

Confocal laser scanning microscopy was performed using an LSM780 (Carl Zeiss, Oberkichen, Germany) equipped with dry objective (20 ×/NA = 0.55), and oil immersion objectives (40 ×/NA = 1.4 or 63 ×/NA = 1.4) or a Leica TCS SP8 confocal laser scanning microscope (Wetzlar, Germany). Five- to-seven-day-old seedlings were observed. Alexander staining was performed as previously described [40], followed by the observation of pollen morphology and viability using a Zeiss Primostar 3 microscope.

The acquired images were processes and analyzed using Fiji [52]. Tracking was performed using TracMate (version: 2.14.0, Fiji) [53]. The estimated particle diameter was set to 1 μm, with a detection threshold of 4 units. Spot detection was performed using the Laplacian of Gaussian (LoG) algorithm, and tracking was conducted using the simple LAP tracker with a maximum linking distance of 10 μm.

Tobacco infiltration Assay

The transient expression in *Nicotiana benthamiana* leaf was performed as described previously [54]. cDNA sequences of *REAP1*, *ARA7*, *ARA6*, *RABA1b* and *RABA6a* were subcloned into the binary vectors pGWB405m or pGWB406m vectors (kind gift from Dr Segami, NIBB, Japan) by Gateway LR reactions. cDNA sequences of *ROP7*, $ROP7^{G15V}$, $ROP7^{T20N}$, *ROP1* and *ROP2*, N-terminally tagged with *mRFP* sequence, were subcloned into pMDC7 by Gateway LR reactions. The expression vectors were introduced into *A. tumefaciens* strain GV3101:pMp90. Agrobacteria were co-infiltrated at OD600 = 0.2 with Agrobacterium carrying the p19 silencing suppressor. β-estradiol (2 μM) was infiltrated 24 hours after the initial infiltration to induce protein expression.

Transient gene expression in Arabidopsis protoplasts

Transient expression of GFP- and/or tagRFP-tagged proteins in Arabidopsis Col-0 suspension cultured cell line (Deep) [55] was conducted as described previously [11,56].

Preparation of wild-type (Col-0) and *reap1* mutant protoplasts and transformation were conducted following a modified protocol of the tape-Arabidopsis sandwich method as described by Wu et al (2009 [57]). Fourteen-day-old roots form Col-0 and *reap1* mutant plants were collected and digested with enzyme solution [1% Cellulase R-10 (Kyowa), 0.25% Pectolyase-Y23 (Kyowa), 0.4 M Mannitol, 10 mM $CaCl_2$, 20 mM KCl, 0.1% BSA, and 20 mM MES (pH5.7)] for 2 hours at room temperature with gentle rotation. The released protoplasts were washed twice with W5 buffer [154 mM NaCl, 125 mM $CaCl_2$, 5 mM KCl, 5 mM glucose, and 2 mM MES (pH5.7)] and resuspended in MMg solution [0.4 M Mannitol, 15 mM MgCl2, and 4 mM MES (pH5.7)]. For transformation, 500 ng or 1 μg plasmid DNA was mixed with 2 μL salmon sperm carrier DNA (Invitrogen, Carlsbad, California, USA) and added to the protoplast suspension, followed by PEG solution [40% PEG6000, 0.1 M $CaCl_2$, and 0.2 M Mannitol]. The mixture was incubated at room temperature for 5 minutes, then washed with W5 buffer. Transformed protoplasts were incubated for two days at 22°C, and then observed by CLSM.

Quantitative real-time PCR

Total RNA was extracted from open flowers of wild-type and *rop7* mutant plants using RNeasy Plant Mini Lit (Qiagen, Hilden, Germany). RNA integrity was evaluated by measuring the absorbance ratio at 260 nm/280 nm. cDNA was synthesized from 500 ng of total RNA by using the ReverTra Ace® qPCR RT Master Mix with gDNA Remover (Toyobo, Osaka, Japan), and the synthesized cDNA was diluted 10-fold for subsequent qRT-PCR analysis. qRT-PCR was performed on a Light Cycler® 96 system (Roche, Basel, Switzerland) with specific primer sets listed in Extended Data Table 4. Each 20 μL reaction mixture contained 2 μL of template cDNA, 0.4 μL of each primer (final concentration: 200 nM each), and 10 μL KAPA SYBR FAST® qPCR Master Mix (2×) (KAPA Biosystems, Boston, Massachusetts, USA). The PCR reaction and the melting curve analysis were conducted following the manufacturer's instructions.

Baseline correction and quantification cycle (Cq) values were automatically calculated using the Light Cycler® 96 software (Roche).

Statistical Analysis

Statistical analyses were performed using R software (version 4.4.2). Normality of data was assessed with the one-sample Kolmogorov-Smirnov test or the Shapiro-Wilk test. Comparisons between two groups were performed using either a two-sided Mann-Whitney U test or a two-sample t-test, depending on the data distribution. For multiple group comparisons, one-way ANOVA was followed by the Tukey-Kramer test as a post-hoc pairwise analysis. Associations between categorical values were analyzed using the chi-squared test or Fisher's exact test, as appropriate. A P value < 0.05 was considered statistically significant. Detailed statistical results are shown in the Extended Data Table 5 or indicated in the figures.

Abbreviations

REAP1 (RAB5 EFFECTOR OF ARABIDOPSIS WITH PH DOMAIN 1), ARA (Arabidopsis Ras-related), Ras (Rat sarcoma), Rho (Ras homology), Rab (Ras-like in brain), Arf (ADP-ribosylation factor), Ran (Ras-like nuclear), SWAP70 (SWITCHING B-CELL COMPLEX ASSOCIATED). PRONE (PLANT-SPECIFIC ROP NUCLEOTIDE EXCHANGER), FAB1 (Formation of aploid and binucleate cells 1)

Declarations

Competing interests

The authors declare no competing interests.

Author contributions

E.I. and T.U. designed the experiments, E.I. performed a major part of the experiments, T.H. and M.H.S. performed the experiment with YM201636, K.E. established the method of transient assay, E.I. and Ta.U. wrote the manuscript, and To.U., A.N. and Ta.U. supervised this work.

Acknowledgements

This work was supported by MEXT KAKENHI Grant Number 19H05670 (to Ta.U.), and 19H05675 (to Ta.U.), JST CREST Grant Number JPMJCR20E5 (to To.U), JSPS KAKENHI Grant Number 21H02515 (to Ta.U.), 24K02050 (to Ta.U.), 22K19327 (to To.U), 22H02643 (to To.U), 15K18527 (to E.I.), 21K06210 (to E.I.), JP24KJ1122 (to E.I.), Takeda Science Foundation (to Ta.U.), Asahi Glass Foundation (to To.U.) and Ito Science Foundation (to E.I.). E.I. was supported by the JSPS through the Research Fellowship for Young Scientists (RPD) (no. 202440124).

References

1. Takai, Y., Sasaki, T. & Matozaki, T. Small GTP-binding proteins. Physiol Rev 81, 153–208, doi:10.1152/physrev.2001.81.1.153 (2001).
2. Wennerberg, K., Rossman, K. L. & Der, C. J. The Ras superfamily at a glance. J Cell Sci 118, 843–846, doi:10.1242/jcs.01660 (2005).
3. Sahai, E., Olson, M. F. & Marshall, C. J. Cross-talk between Ras and Rho signalling pathways in transformation favours proliferation and increased motility. EMBO J 20, 755–766, doi:10.1093/emboj/20.4.755 (2001).
4. Nik Akhtar, S., Bunner, W. P., Brennan, E., Lu, Q. & Szatmari, E. M. Crosstalk between the Rho and Rab family of small GTPases in neurodegenerative disorders. Front Cell Neurosci 17, 1084769, doi:10.3389/fncel.2023.1084769 (2023).
5. Saito, C. & Ueda, T. Chapter 4: functions of RAB and SNARE proteins in plant life. Int Rev Cell Mol Biol 274, 183–233, doi:10.1016/S1937-6448(08)02004-2 (2009).
6. Ueda, T. & Nakano, A. Vesicular traffic: an integral part of plant life. Curr Opin Plant Biol 5, 513–517, doi:10.1016/s1369-5266(02)00299-6 (2002).
7. Rutherford, S. & Moore, I. The Arabidopsis Rab GTPase family: another enigma variation. Curr Opin Plant Biol 5, 518–528, doi:10.1016/s1369-5266(02)00307-2 (2002).
8. Pereira-Leal, J. B. & Seabra, M. C. Evolution of the Rab family of small GTP-binding proteins. J Mol Biol 313, 889–901, doi:10.1006/jmbi.2001.5072 (2001).
9. Ito, E. & Uemura, T. RAB GTPases and SNAREs at the trans-Golgi network in plants. J Plant Res 135, 389–403, doi:10.1007/s10265-022-01392-x (2022).
10. Minamino, N. & Ueda, T. RAB GTPases and their effectors in plant endosomal transport. Curr Opin Plant Biol 52, 61–68, doi:10.1016/j.pbi.2019.07.007 (2019).
11. Ueda, T., Yamaguchi, M., Uchimiya, H. & Nakano, A. Ara6, a plant-unique novel type Rab GTPase, functions in the endocytic pathway of Arabidopsis thaliana. EMBO J 20, 4730–4741, doi:10.1093/emboj/20.17.4730 (2001).
12. Ito, E., Uemura, T., Ueda, T. & Nakano, A. Distribution of RAB5-positive multivesicular endosomes and the trans-Golgi network in root meristematic cells of Arabidopsis thaliana. Plant Biotechnol (Tokyo) 33, 281–286, doi:10.5511/plantbiotechnology.16.0218a (2016).
13. Ito, E. *et al.* Integration of two RAB5 groups during endosomal transport in plants. Elife 7, doi:10.7554/eLife.34064 (2018).
14. Ebine, K. *et al.* A membrane trafficking pathway regulated by the plant-specific RAB GTPase ARA6. Nat Cell Biol 13, 853–859, doi:10.1038/ncb2270 (2011).
15. Brembu, T., Winge, P., Bones, A. M. & Yang, Z. A RHOse by any other name: a comparative analysis of animal and plant Rho GTPases. Cell Res 16, 435–445, doi:10.1038/sj.cr.7310055 (2006).
16. Oda, Y. & Fukuda, H. Initiation of cell wall pattern by a Rho- and microtubule-driven symmetry breaking. Science 337, 1333–1336, doi:10.1126/science.1222597 (2012).

17. Engelhardt, S., Trutzenberg, A. & Huckelhoven, R. Regulation and Functions of ROP GTPases in Plant-Microbe Interactions. Cells 9, doi:10.3390/cells9092016 (2020).
18. Denninger, P. RHO OF PLANTS signalling and the activating ROP GUANINE NUCLEOTIDE EXCHANGE FACTORS: specificity in cellular signal transduction in plants. J Exp Bot 75, 3685–3699, doi:10.1093/jxb/erae196 (2024).
19. Rossman, K. L., Der, C. J. & Sondek, J. GEF means go: turning on RHO GTPases with guanine nucleotide-exchange factors. Nat Rev Mol Cell Biol 6, 167–180, doi:10.1038/nrm1587 (2005).
20. Yamaguchi, K. *et al.* SWAP70 functions as a Rac/Rop guanine nucleotide-exchange factor in rice. Plant J 70, 389–397, doi:10.1111/j.1365-313X.2011.04874.x (2012).
21. van Leeuwen, W., Okresz, L., Bogre, L. & Munnik, T. Learning the lipid language of plant signalling. Trends Plant Sci 9, 378–384, doi:10.1016/j.tplants.2004.06.008 (2004).
22. Thole, J. M. & Nielsen, E. Phosphoinositides in plants: novel functions in membrane trafficking. Curr Opin Plant Biol 11, 620–631, doi:10.1016/j.pbi.2008.10.010 (2008).
23. Heilmann, I. Phosphoinositide signaling in plant development. Development 143, 2044–2055, doi:10.1242/dev.136432 (2016).
24. Arcaro, A. & Wymann, M. P. Wortmannin is a potent phosphatidylinositol 3-kinase inhibitor: the role of phosphatidylinositol 3,4,5-trisphosphate in neutrophil responses. Biochem J 296 (Pt 2), 297–301, doi:10.1042/bj2960297 (1993).
25. Yano, H. *et al.* Inhibition of histamine secretion by wortmannin through the blockade of phosphatidylinositol 3-kinase in RBL-2H3 cells. J Biol Chem 268, 25846–25856 (1993).
26. Matsuoka, K., Bassham, D. C., Raikhel, N. V. & Nakamura, K. Different sensitivity to wortmannin of two vacuolar sorting signals indicates the presence of distinct sorting machineries in tobacco cells. J Cell Biol 130, 1307–1318, doi:10.1083/jcb.130.6.1307 (1995).
27. Nakanishi, S., Catt, K. J. & Balla, T. A wortmannin-sensitive phosphatidylinositol 4-kinase that regulates hormone-sensitive pools of inositolphospholipids. Proc Natl Acad Sci U S A 92, 5317–5321, doi:10.1073/pnas.92.12.5317 (1995).
28. Jung, J. Y. *et al.* Phosphatidylinositol 3- and 4-phosphate are required for normal stomatal movements. Plant Cell 14, 2399–2412, doi:10.1105/tpc.004143 (2002).
29. Jefferies, H. B. *et al.* A selective PIKfyve inhibitor blocks PtdIns(3,5)P(2) production and disrupts endomembrane transport and retroviral budding. EMBO Rep 9, 164–170, doi:10.1038/sj.embor.7401155 (2008).
30. Hirano, T., Munnik, T. & Sato, M. H. Phosphatidylinositol 3-Phosphate 5-Kinase, FAB1/PIKfyve Kinase Mediates Endosome Maturation to Establish Endosome-Cortical Microtubule Interaction in Arabidopsis. Plant Physiol 169, 1961–1974, doi:10.1104/pp.15.01368 (2015).
31. Goh, T. *et al.* VPS9a, the common activator for two distinct types of Rab5 GTPases, is essential for the development of Arabidopsis thaliana. Plant Cell 19, 3504–3515, doi:10.1105/tpc.107.053876 (2007).

32. Dettmer, J., Hong-Hermesdorf, A., Stierhof, Y. D. & Schumacher, K. Vacuolar H+-ATPase activity is required for endocytic and secretory trafficking in Arabidopsis. Plant Cell 18, 715–730, doi:10.1105/tpc.105.037978 (2006).
33. Uemura, T. *et al.* Qa-SNAREs localized to the trans-Golgi network regulate multiple transport pathways and extracellular disease resistance in plants. Proc Natl Acad Sci U S A 109, 1784–1789, doi:10.1073/pnas.1115146109 (2012).
34. McCloud, T. G. *et al.* Production of brefeldin-A. J Ind Microbiol 15, 5–9, doi:10.1007/BF01570006 (1995).
35. Chardin, P. & McCormick, F. Brefeldin A: the advantage of being uncompetitive. Cell 97, 153–155, doi:10.1016/s0092-8674(00)80724-2 (1999).
36. Grebe, M. *et al.* Arabidopsis sterol endocytosis involves actin-mediated trafficking via ARA6-positive early endosomes. Curr Biol 13, 1378–1387, doi:10.1016/s0960-9822(03)00538-4 (2003).
37. Yamaguchi, K. & Kawasaki, T. Function of Arabidopsis SWAP70 GEF in immune response. Plant Signal Behav 7, 465–468, doi:10.4161/psb.19562 (2012).
38. Feiguelman, G., Fu, Y. & Yalovsky, S. ROP GTPases Structure-Function and Signaling Pathways. Plant Physiol 176, 57–79, doi:10.1104/pp.17.01415 (2018).
39. Bloch, D. & Yalovsky, S. Cell polarity signaling. Curr Opin Plant Biol 16, 734–742, doi:10.1016/j.pbi.2013.10.009 (2013).
40. Alexander, M. P. Differential staining of aborted and nonaborted pollen. Stain Technol 44, 117–122, doi:10.3109/10520296909063335 (1969).
41. Wang, W. *et al.* The RopGEF2-ROP7/ROP2 Pathway Activated by phyB Suppresses Red Light-Induced Stomatal Opening. Plant Physiol 174, 717–731, doi:10.1104/pp.16.01727 (2017).
42. Cao, C. *et al.* Corrigendum to: Phosphatidic acid binds to and regulates guanine nucleotide exchange factor 8 (GEF8) activity in Arabidopsis. Funct Plant Biol 48, 359, doi:10.1071/FP17113_CO (2021).
43. Ryu, K. H., Huang, L., Kang, H. M. & Schiefelbein, J. Single-Cell RNA Sequencing Resolves Molecular Relationships Among Individual Plant Cells. Plant Physiol 179, 1444–1456, doi:10.1104/pp.18.01482 (2019).
44. Higa, T. *et al.* Microtubule-associated phase separation of MIDD1 tunes cell wall spacing in xylem vessels in Arabidopsis thaliana. Nat Plants 10, 100–117, doi:10.1038/s41477-023-01593-9 (2024).
45. Kawashima, T. *et al.* Dynamic F-actin movement is essential for fertilization in Arabidopsis thaliana. Elife 3, doi:10.7554/eLife.04501 (2014).
46. Ivanchenko, M., Vejlupkova, Z., Quatrano, R. S. & Fowler, J. E. Maize ROP7 GTPase contains a unique, CaaX box-independent plasma membrane targeting signal. Plant J 24, 79–90, doi:10.1046/j.1365-313x.2000.00855.x (2000).
47. Brembu, T., Winge, P. & Bones, A. M. The small GTPase AtRAC2/ROP7 is specifically expressed during late stages of xylem differentiation in Arabidopsis. J Exp Bot 56, 2465–2476, doi:10.1093/jxb/eri239 (2005).

48. Kawasaki, T. *et al.* The small GTP-binding protein rac is a regulator of cell death in plants. Proc Natl Acad Sci U S A 96, 10922–10926, doi:10.1073/pnas.96.19.10922 (1999).
49. Gehl, C., Waadt, R., Kudla, J., Mendel, R. R. & Hansch, R. New GATEWAY vectors for high throughput analyses of protein-protein interactions by bimolecular fluorescence complementation. Mol Plant 2, 1051–1058, doi:10.1093/mp/ssp040 (2009).
50. Francis, K. E., Lam, S. Y. & Copenhaver, G. P. Separation of Arabidopsis pollen tetrads is regulated by QUARTET1, a pectin methylesterase gene. Plant Physiol 142, 1004–1013, doi:10.1104/pp.106.085274 (2006).
51. Inada, N. *et al.* Modulation of Plant RAB GTPase-Mediated Membrane Trafficking Pathway at the Interface Between Plants and Obligate Biotrophic Pathogens. Plant Cell Physiol 57, 1854–1864, doi:10.1093/pcp/pcw107 (2016).
52. Schindelin, J. *et al.* Fiji: an open-source platform for biological-image analysis. Nat Methods 9, 676–682, doi:10.1038/nmeth.2019 (2012).
53. Ershov, D. *et al.* TrackMate 7: integrating state-of-the-art segmentation algorithms into tracking pipelines. Nat Methods 19, 829–832, doi:10.1038/s41592-022-01507-1 (2022).
54. Choi, S. W. *et al.* RABA members act in distinct steps of subcellular trafficking of the FLAGELLIN SENSING2 receptor. Plant Cell 25, 1174–1187, doi:10.1105/tpc.112.108803 (2013).
55. Mathur, J. *et al.* Gene identification with sequenced T-DNA tags generated by transformation of Arabidopsis cell suspension. Plant J 13, 707–716, doi:10.1046/j.1365-313x.1998.00059.x (1998).
56. Uemura, T. *et al.* Systematic analysis of SNARE molecules in Arabidopsis: dissection of the post-Golgi network in plant cells. Cell Struct Funct 29, 49–65, doi:10.1247/csf.29.49 (2004).
57. Wu, F. H. *et al.* Tape-Arabidopsis Sandwich - a simpler Arabidopsis protoplast isolation method. Plant Methods 5, 16, doi:10.1186/1746-4811-5-16 (2009).

Figures

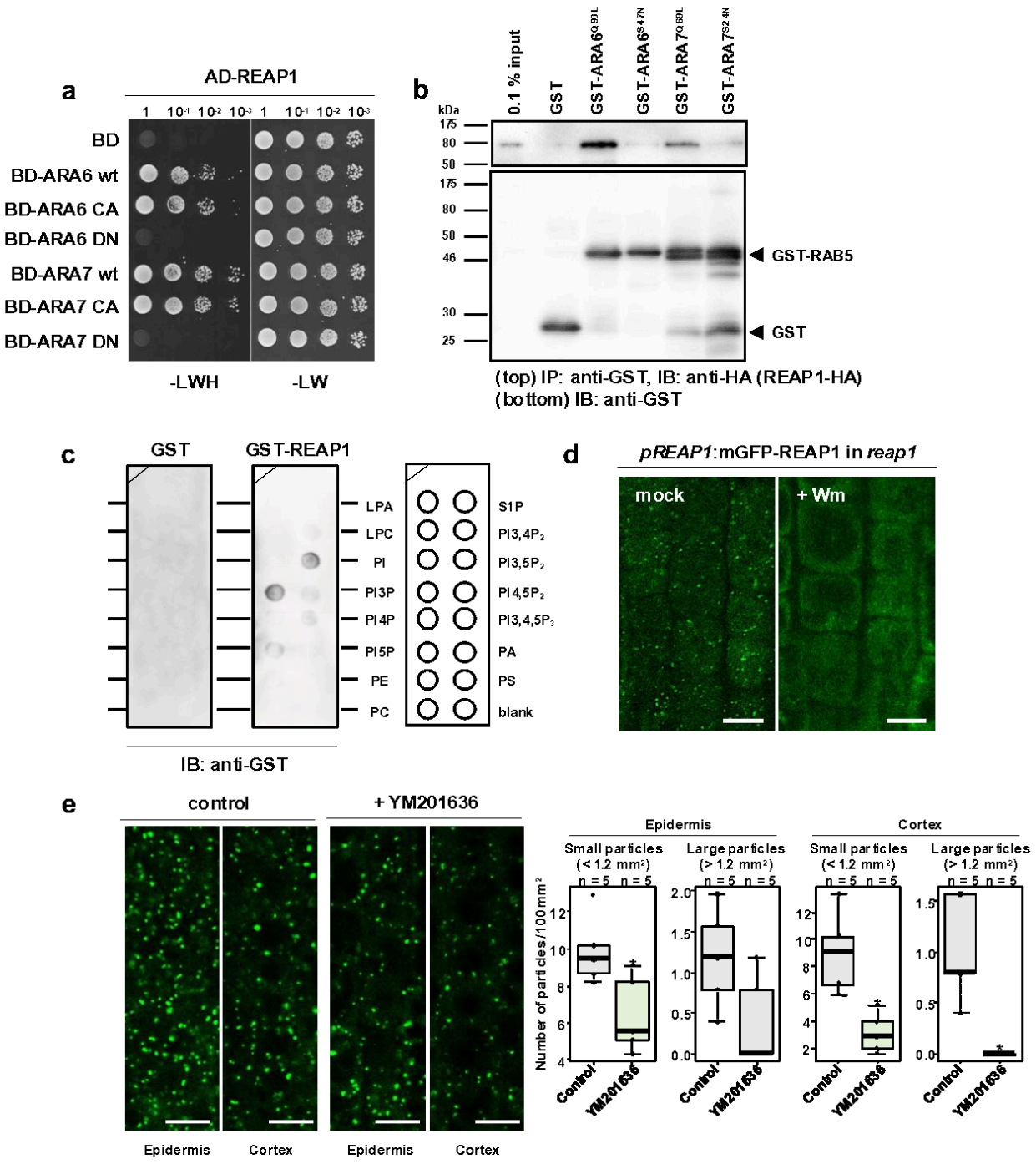


Figure 1

REAP1/AtSWAP70 binds to active RAB5s, PI3P and PI3,5P_2

a. Yeast two-hybrid interaction between REAP1 and RAB5s (ARA6 or ARA7). REAP1 was expressed as a fusion protein with the activation domain (AD), while wild-type (WT), constitutively active (CA), and dominant negative (DN) ARA6 and ARA7 were expressed as fusion proteins with the DNA binding

domain (BD) in yeast strain AH109. Interaction was assessed by activation of *HIS3* reporter gene expression.

b. In vitro pull-down assay demonstrating the interaction between REAP1 and RAB5s. GST-tagged RAB5 proteins in GTP- or GDP-bound state were used to pull down REAP1 expressed in yeast.

c. Lipid binding assay. GST-tagged REAP1 was incubated with the lipid-spotted membrane and bound protein was detected with an anti-GST antibody.

d. Effect of wortmannin (Wm) on REAP1 localization. REAP1 predominantly localized to punctate structures in root epidermal cells. Five-day-old seedlings were treated with 33 μM Wm for 2 hours and observed under CLSM. Bars = 10 μm.

e. Effect of YM201636 on REAP1 localization. The number of punctate GFP-REAP1 signals in root epidermal and cortical cells was quantified in the presence or absence of 100 nM YM201636. Bars = 10 μm. In the box-and-whisker plots, boxes represent the interquartile (25^{th} to 75^{th} percentiles), solid lines within the boxes indicate median values, and whiskers denote the 95% confidence intervals. Significant differences ($P < 0.05$; indicated by asterisks) were determined using the Mann-Whitney U-test. The “n” values indicate the number of independent root cell samples analyzed.

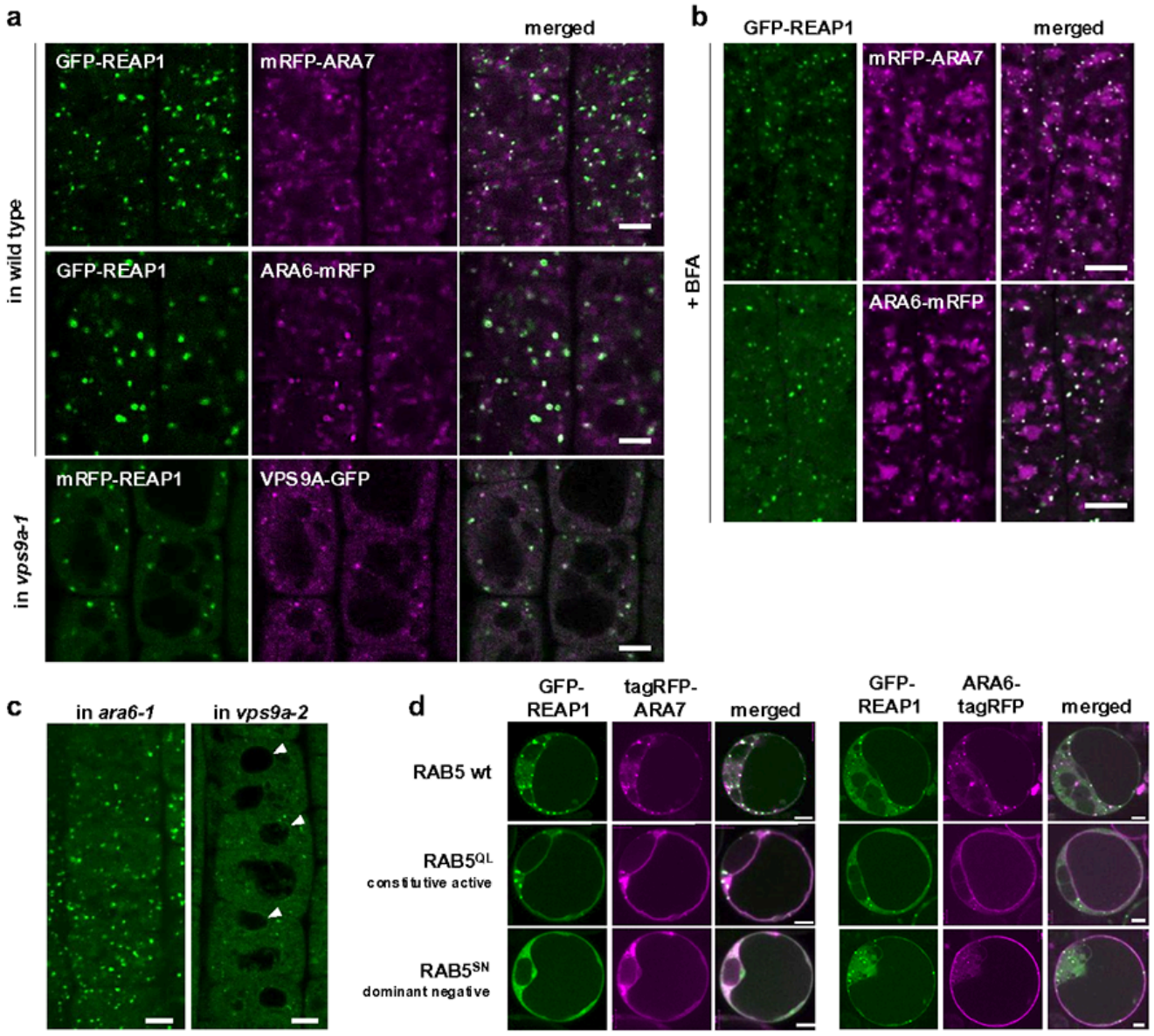


Figure 2

REAP1 localizes to multivesicular endosomes (MVEs) in a canonical RAB5-dependent manner.

a. Localization patterns of GFP-REAP1 or mRFP-REAP1 in relation to mRFP-tagged ARA7 and ARA6 or GFP-tagged VPS9A. REAP1 signals were observed to overlap with ARA7, ARA6, and VPS9A signals in root epidermal cells. Bars = 5 μm.

b. Effect of BFA treatment on REAP1-positive MVEs. Five-day-old seedlings were treated with 50 μM BFA for 30 minutes, and the root epidermal cells were observed under CLSM. REAP1-positive MVEs were not

observed to be incorporated into BFA bodies. Bars = 10 μm.

c. Subcellular localization of REAP1 in the *ara6-1* and *vps9a-2* mutants. In the *ara6-1* mutant, REAP1 localized to punctate structures similar to those observed in wild-type plants. In the *vps9a-2* mutant, the REAP1 signal was distributed throughout the cytosol, with a faint signal on the vacuolar membrane (arrowheads). Bars = 10 μm.

d. Effect of expression of constitutively active or dominant negative RAB5 on the subcellular localization of REAP1. GFP-REAP1 localizes to punctate structures in protoplasts when coexpressed with tagRFP-tagged ARA7, ARA7^{Q69L}, ARA6, ARA6^{Q93L}, or ARA6^{S47N}, whereas GFP-REAP1 signal was dispersed into the cytosol when coexpressed with tagRFP-ARA7^{S24N}. Bars = 5 μm.

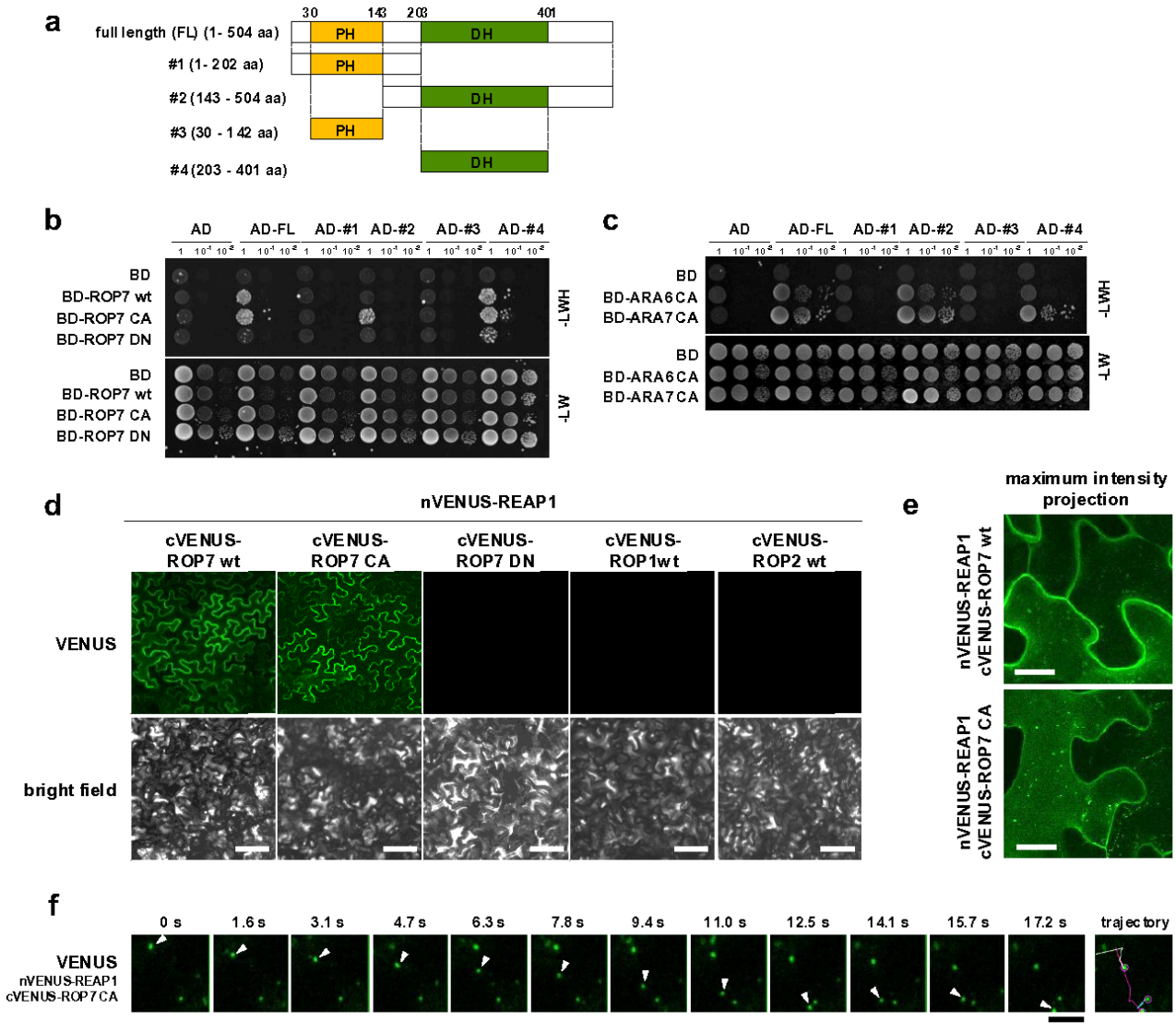


Figure 3

REAP1 interacts with active ROP7.

a. Schematic representation of full length and truncated REAP1 constructs used for interaction assays.

b. Yeast two-hybrid interactions between full-length or truncated REAP1 and ROP7. REAP1 was fused to the AD and wild-type (wt), constitutively active (CA), or dominant negative (DN) ROP7 fused to the BD were co-expressed in yeast strain AH109. Interaction was assessed by activation of *HIS3*reporter gene expression.

c. Yeast two-hybrid interaction between full length or truncated REAP1 and RAB5s (ARA6 and ARA7). Truncated REAP1 was fused to the AD and constitutively active (CA) RAB5s were fused to the BD. Interaction was assessed by activation of *HIS3* reporter gene expression.

d. Bimolecular fluorescence complementation (BiFC) analysis of REAP1 and ROP7 interaction in *Nicotiana benthamiana* leaf epidermal cells. Fluorescence from reconstituted VENUS, indicating the interaction, was observed for wild-type and constitutively active (CA) ROP7, but not for dominant negative (DN) ROP7 or wild-type ROP1 and ROP2. Bar = 100 μm.

e. Maximum intensity projection images of *N. benthamiana* leaf epidermal cells expressing nVENUS-tagged REAP1 and cVENUS-tagged wild-type or constitutively active ROP7. Bars = 20 μm.

f. Sequential confocal images showing dynamic movement of puncta visualized by the interaction between REAP1 and constitutively active ROP7. Puncta moved along with cytoplasmic streaming. The rightmost panel shows the trajectory (pink) of a representative punctum (arrowhead). Bar = 5 μm.

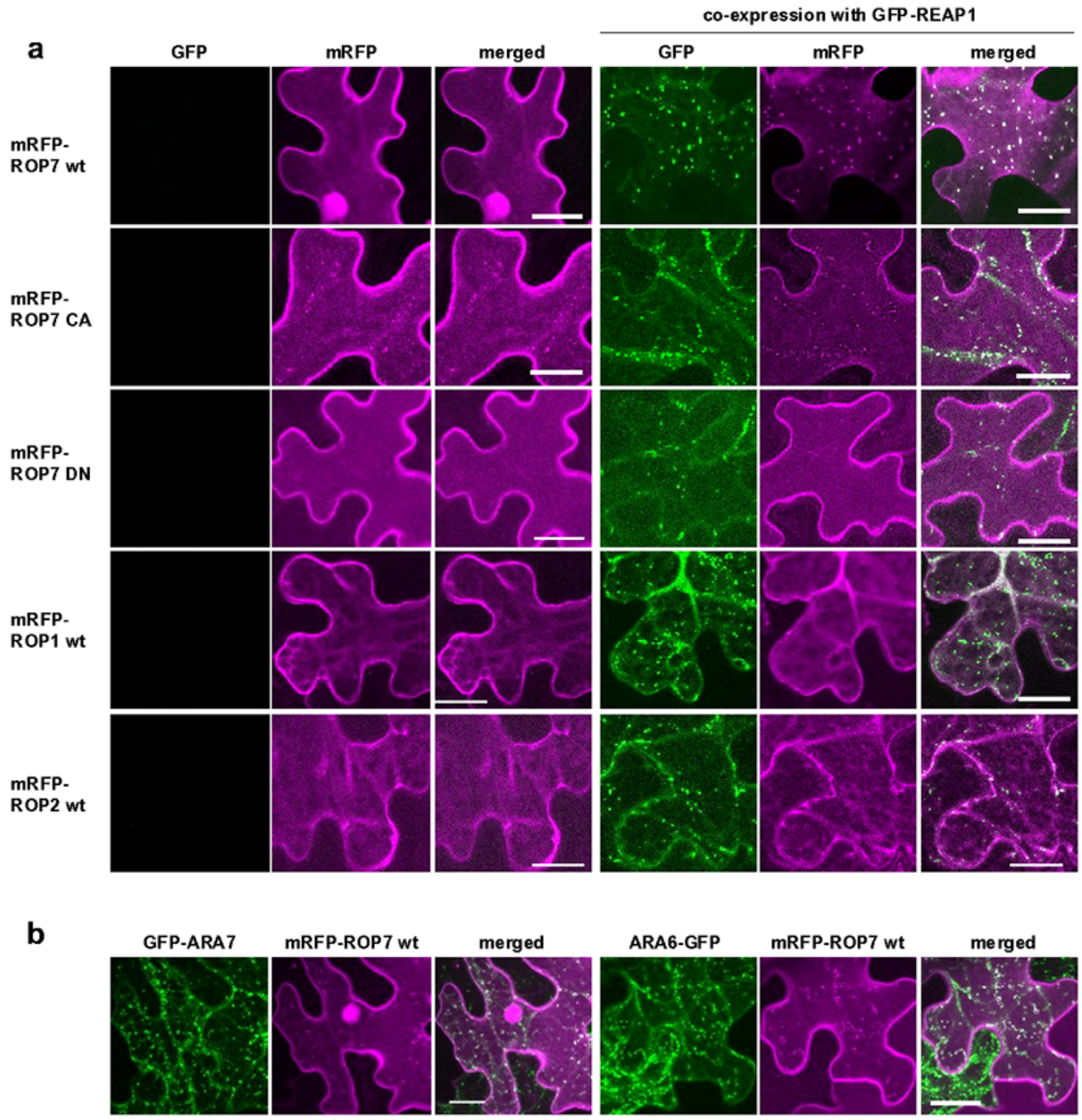


Figure 4

Overexpression of REAP1, ARA7, or ARA6 recruits ROP7 to MVEs.

a. Maximum intensity projection images of *N. benthamiana* leaf epidermal cells expressing mRFP-tagged wild-type, constitutively active (CA), or dominant negative (DN) ROP7 or ROP1 or ROP2 with or without GFP-tagged REAP1. mRFP-tagged ROPs localize primarily to the plasma membrane, whereas punctate localization of wild-type and CA ROP7 was evident when coexpressed with REAP1. Bars = 20 μm.

b. Maximum intensity projection images of *N. benthamiana* leaf epidermal cells coexpressing mRFP-tagged wild-type ROP7 and GFP-tagged ARA7 or ARA6. ROP7 colocalized with ARA7 and ARA6 at punctate structures. Bars = 20 μm.

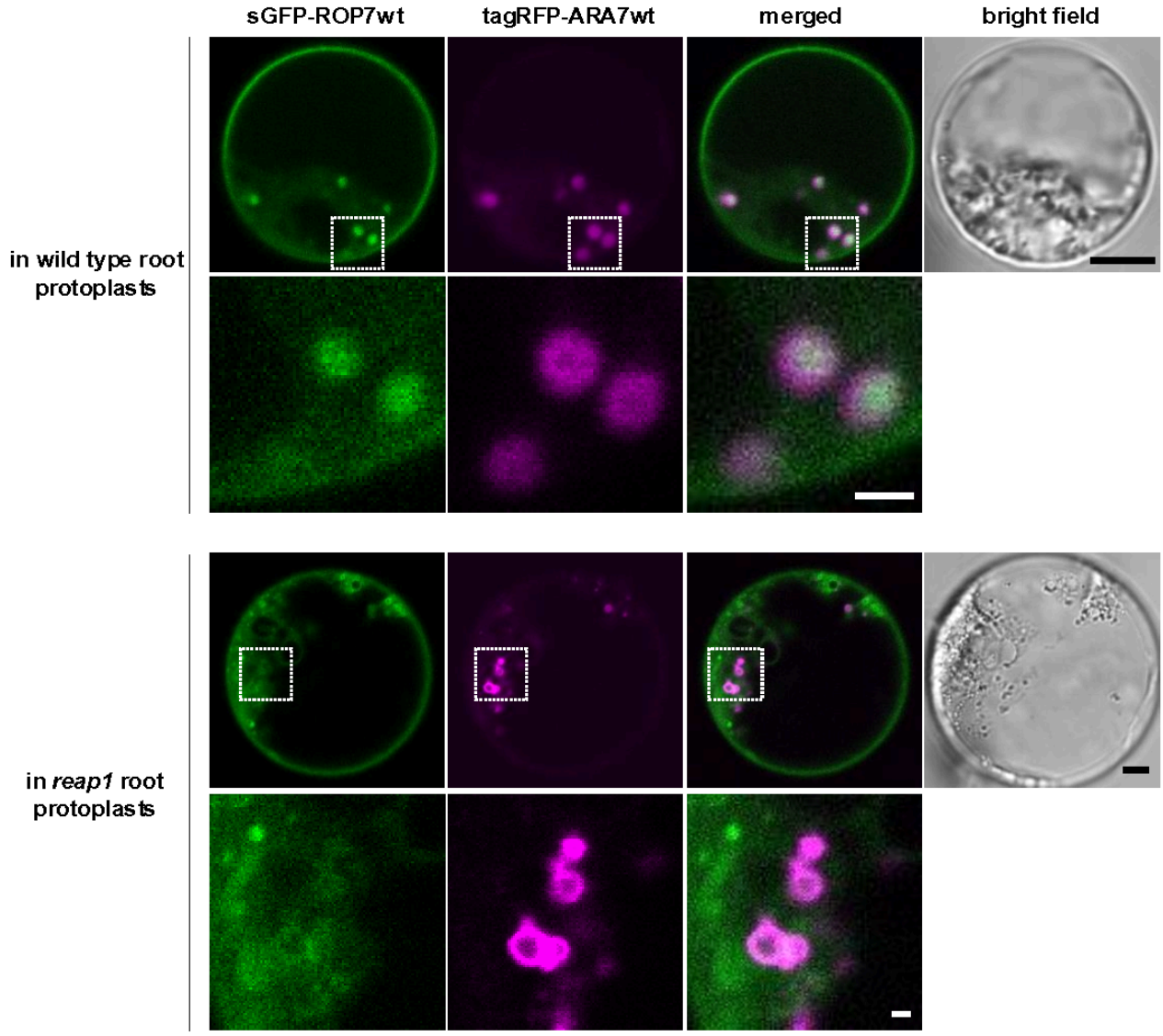


Figure 5

Recruitment of ROP7 to endosomes by ARA7 requires REAP1.

Localization of GFP-tagged ROP7 co-expressed with tagRFP-ARA7 in protoplasts prepared from wild-type (top panels) or *reap1*mutant (bottom panels) roots. Bar = 5 μm. Magnified views of the boxed regions are also shown. Bar = 1 μm.

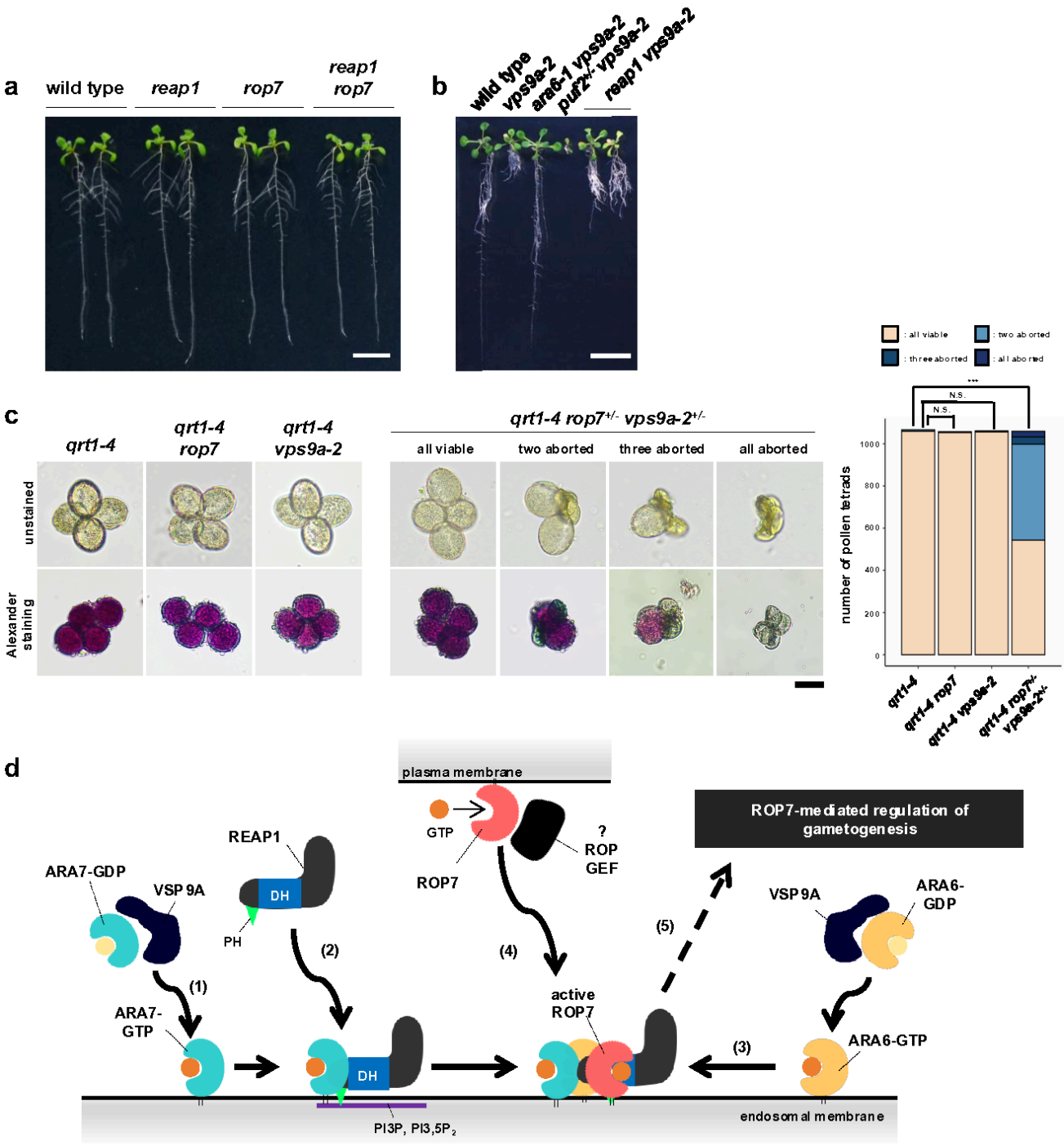


Figure 6

The RAB5-REAP1-ROP7 cascade is involved in gametogenesis.

a. Genetic interaction between *REAP1* and *ROP7* during vegetative growth. Ten-day-old plants are shown. Bar = 1 cm.

b. Genetic interaction between *REAP1* and *VPS9A* during vegetative growth. Fourteen-day-old plants are shown. Bar = 1 cm.

c. Morphology and viability of pollen tetrads from *qrt1-4*, *qrt1-4 rop7*, *qrt1-4 vps9a-2*, and *qrt1-4 rop7*$^{+/-}$ *vps9a-2*$^{+/-}$ mutant flowers. Upper panels show pollen tetrad morphology, and lower panels show viability assessed by Alexander staining. Bar = 20 μm. The graph quantifies the number of pollen tetrads with the indicated abortion patterns. The ratios of “all viable” : “two aborted”: “three aborted” : “all aborted” were as follows: for *qrt1-4*, 1059 : 7: 0 : 0 (n = 1066 pollen tetrads), for *qrt1-4 rop7*, 1053 : 4 : 0 : 0 (n = 1057 pollen tetrads), for *qrt1-4 vps9a-2*, 1056 : 5 : 0 : 0 (n = 1061 pollen tetrads), and for *qrt1-4 rop7*$^{+/-}$ *vps9a-2*$^{+/-}$, 543 : 455 : 34 : 27 (n = 1059 pollen tetrads). ****P* < 0.01, NS = not significant by Fisher’s exact test.

d. Proposed model for the RAB5-REAP1-ROP7 cascade. Canonical RAB7 (ARA7 in this figure) is activated by VPS9A, which localizes activated ARA7 to the endosomal membrane (1). This in turn recruits REAP1 to endosomes (2). The PH domain of REAP1 stabilizes its endosomal localization by binding to PI3P and PI3,5P_2 in the endosomal membrane. ARA6, which is also activated by VPS9A, binds to REAP1 on endosomes (3). ROP7 on the plasma membrane is activated by an unidentified ROP GEF, and the active form of ROP7 is recruited to the endosomal membrane by REAP1 (4). ROP7 on endosomes transduces signals to regulate processes such as gametogenesis (5).

Supplementary Files

This is a list of supplementary files associated with this preprint. Click to download.

- ExtendedDataTablesfinal2.pdf
- ExtendedDataMovie1.mp4
- ExtendedDataMovie2.mp4
- ExtendedDataMovie3.mp4